Theoretical Notes
Note 268

UNCLASSIFIED

SECURITY CLASSIFICATION OF THIS PAGE *(When Data Entered)*

REPORT DOCUMENTATION PAGE		READ INSTRUCTIONS BEFORE COMPLETING FORM
1. REPORT NUMBER SAMSO-TR-75-295	2. GOVT ACCESSION NO.	3. RECIPIENT'S CATALOG NUMBER
4. TITLE *(and Subtitle)* FORWARD AND BACKWARD PHOTO-EMISSION YIELDS FROM METALS AT VARIOUS X-RAY ANGLES OF INCIDENCE		5. TYPE OF REPORT & PERIOD COVERED Interim 6. PERFORMING ORG. REPORT NUMBER TR-0076(6250-30)-1
7. AUTHOR(s) Melvin J. Bernstein and Kenneth W. Paschen		8. CONTRACT OR GRANT NUMBER(s) F04701-75-C-0076
9. PERFORMING ORGANIZATION NAME AND ADDRESS The Aerospace Corporation El Segundo, Calif. 90245		10. PROGRAM ELEMENT, PROJECT, TASK AREA & WORK UNIT NUMBERS
11. CONTROLLING OFFICE NAME AND ADDRESS Space and Missile Systems Organization Air Force Systems Command Los Angeles, Calif. 90009		12. REPORT DATE 16 December 1975 13. NUMBER OF PAGES 26
14. MONITORING AGENCY NAME & ADDRESS*(if different from Controlling Office)*		15. SECURITY CLASS. *(of this report)* Unclassified 15a. DECLASSIFICATION/DOWNGRADING SCHEDULE

16. DISTRIBUTION STATEMENT *(of this Report)*

Approved for public release; distribution unlimited.

17. DISTRIBUTION STATEMENT *(of the abstract entered in Block 20, if different from Report)*

18. SUPPLEMENTARY NOTES

19. KEY WORDS *(Continue on reverse side if necessary and identify by block number)*

X-ray photoemission
Photoelectrons
Electron photoemission
Secondary electrons

20. ABSTRACT *(Continue on reverse side if necessary and identify by block number)*

X-ray generated photoemission from thin metal foils backed by graphite was measured with radiation incident from the front and back sides at several angles. Irradiation was provided by a 100-kV x-ray tube with three different filters to harden the spectrum. The total 2π photoelectron emission current from a surface was measured. A biased grid retarded the low-energy secondary electrons that added only 10 to 30% to the current at zero grid bias. Investigated metals were: Mg, Al, Ti, Fe, Cu, Ag, Ta, Au, and Pb. The

DD FORM (FACSIMILE) 1473

UNCLASSIFIED

SECURITY CLASSIFICATION OF THIS PAGE *(When Data Entered)*

19. KEY WORDS *(Continued)*

20. ABSTRACT *(Continued)*

total emission from the graphite support only was measured. It was determined that the front-to-back ratio of emission currents at normal incidence ranged from about 1.9 for Al and Mg down to about 1.1 for Ta. The photoelectron yield was found to be $G_e \mu_a S_e$ electrons/photon, where μ_a and S_e are the energy-dependent photon absorption cross section and computed electron mean path length in the emitter and G_e is a constant that is assumed to be independent of photon energy in the range studied but which depends on the radiation angle of incidence. For the photon energy range of 20 to 70 keV, the measured emission current densities corresponded to the following average values for $\overline{G}_e$: 0.37 ± 0.06 for C, 0.30 ± 0.03 for Al, 0.21 ± 0.02 for Cu and Ag, and 0.18 ± 0.02 for Ta.

CONTENTS

FIGURES

TABLES

I. INTRODUCTION

Many theoretical and experimental studies have been conducted to determine the properties of photoemission from metal surfaces where the energies of the incident photons have varied greatly from a few eV to over a MeV. Electron emission by photons in the 10 to 100-keV range is of interest because the photoelectrons originate in a layer much thicker than the usual complex surface films, and yet these electrons are generated primarily by the photoelectric effect rather than by Compton scattering. When one ignores the contribution of low-energy secondary electrons, the photoemission yield from a surface depends on a combination of four effects: (a) electron-production cross sections, (b) electron mean path lengths, (c) initial electron velocity distributions in space and energy, and (d) electron scattering. In general, depending on the interplay of the last two effects, this photoemission yield will vary for different radiation angles of incidence. For comparison with theory, other recent experiments were directed toward detailed determinations of the electron energy distribution and fluence at just a very few selected angles for the incident radiation and emitted electrons.[1] In the present study, the total photoemission current from one side of a metal foil backed by graphite was measured for radiation incident from the forward and backward directions at several angles. Since previous studies indicate that photoemission from a flat surface has approximately a cos θ angular dependence, we did not attempt any angular resolution. In addition, there was no energy resolution except to retard the very low-energy secondary electrons. In some ways, this study is an extension of our previously reported results of pulsed photoemission from polymers and some metals.[2]

---

[1] J. N. Bradford, "Absolute Yields of X-Ray Induced Photoemission from Metals," IEEE Trans. Nucl. Sci. NS-19, 167 (1972).

[2] F. Hai and M. J. Bernstein, "Photoemission from Polymers," IEEE Trans. Nucl. Sci. NS-18, 178 (1971).

The aspects emphasized in the present work were the relative photoemission at several radiation angles of incidence, the comparison of forward and backward photoemission, and the photoemission yield for many materials ranging from carbon to lead.

II. EXPERIMENTAL SETUP AND PROCEDURE

The experimental arrangement used for the photoemission measurements is shown in Fig. 1. The X-radiation from a steady-state source entered an aluminum vacuum chamber with an i.d. of 27 cm, and photoelectrons were emitted from target foils suspended on the chamber axis. Each thin target was taped flat to a 0.15-cm thick graphite support sheet hung from a rotatable electrical feedthrough, and the electron emission currents were measured with an electrometer. These photocurrents were measured using an input resistance of 10^{10} ohms, and signals of 1 to 1000 millivolts were obtained. Graphite was used for the target support because of its very low photoemission. As will be shown, the photoemission increases rapidly with increased atomic number z (approximately as z^3). Although the photoemission from beryllium should be even less than from graphite, the thick oxide coating on some Be samples produced a higher photoemission.

A lead collimator on the entrance window of the vacuum chamber limited the beam divergence to a full angle of 6.4 deg, which allowed an illuminated diameter of 3.2 cm on the chamber axis 28.5 cm from the x-ray source. Two target sizes were used. Initially, the graphite support and target foils were 15 cm wide, so that 90% of the incident beam still hit the foil at an oblique angle of 80 deg to the surface normal. This provided very large signals at oblique incidence, but at normal incidence there was excessive collection of secondary electrons off the chamber wall. Consequently, subsequent tests utilized a target only 2.5 cm wide so that about the same foil area was irradiated at all angles of incidence. For this latter case, photoemission from a Ta strip only 0.6 cm wide was also measured to provide a small geometric correction factor. A bias grid with an average diameter of 22 cm and a transparency of about 95% was located inside the vacuum chamber to retard low-energy secondary electrons emitted from the foils. Data were obtained with no bias potential and with bias potentials ranging from ±1 to ±1000 volts. The grid wires were oriented so that no radiation was

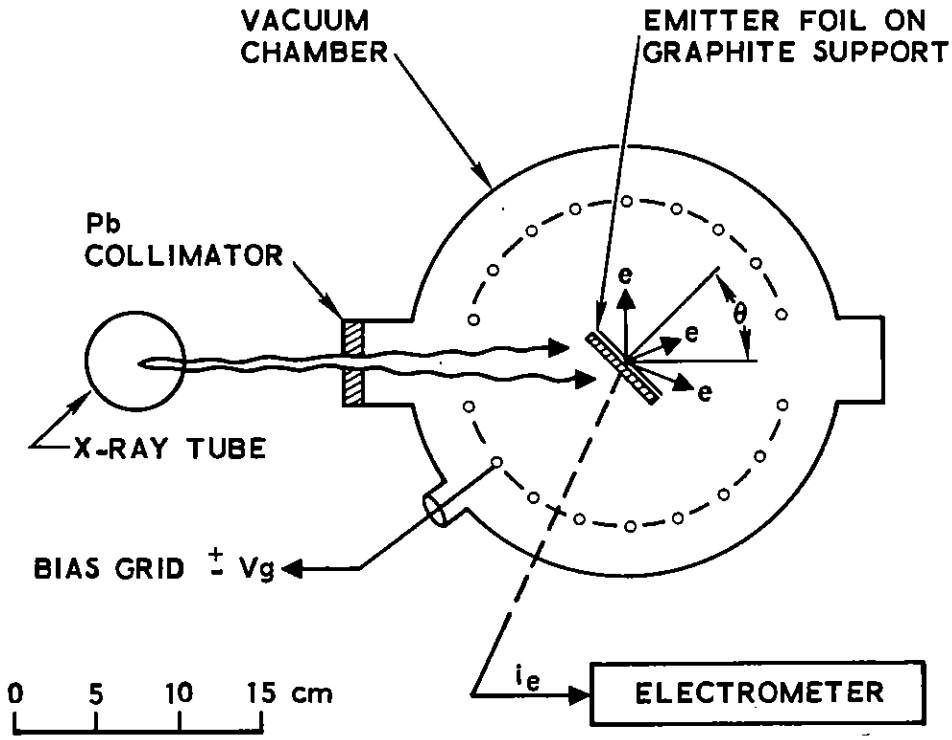

Fig. 1. Schematic Diagram of Apparatus to Measure X-Ray Photoemission from Thin Metal Foils in Forward and Backward Directions

incident on them. In addition, the radiation entrance and exit windows were coated with carbon in the form of aquadaq to minimize photoemission off the chamber wall.

The radiation source was a 160-kV Machlett x-ray tube connected to a 120-kV dc power supply. For the present measurements, the tube was operated at 100 kV and 1 mA. Attenuation of the radiation passing through the pyrex wall of the x-ray tube and two thin windows before striking the target was equivalent to a filter of 0.72 gm/cm^2 aluminum. To obtain additional data, we also added copper filters with thicknesses of 0.25 and 0.59 gm/cm^2 to harden the radiation spectrum. The unfiltered x-ray spectrum was assumed to be an average of the spectra measured at 100 kV on three different devices at LASL,[3] and the calculated attenuation in the filters resulted in the three irradiation spectra shown in Fig. 2. As a check, dose rates were measured using a PIN silicon diode and compared to calculated dose rates. The photon flux was also measured using a NaI detector behind a small aperture in 8-mm lead. The light pulses were detected by a photomultiplier and counted on a scaler; only limited energy discrimination was used. Both measurements agreed with the assumed spectra to about ±15%. An error of about ±5% was introduced in the relative measurements of each foil because of inaccuracies in resetting the voltage and current applied to the x-ray tube and fluctuations in the power supply output.

[3] E. Storm, H. I. Israel, and D. W. Lier, Bremsstrahlung Emission Measurement from Thick Tungsten Targets in the Energy Range 12 to 300 kV, LA-4624, Los Alamos Scientific Laboratory, Los Alamos, New Mexico (April 1971).

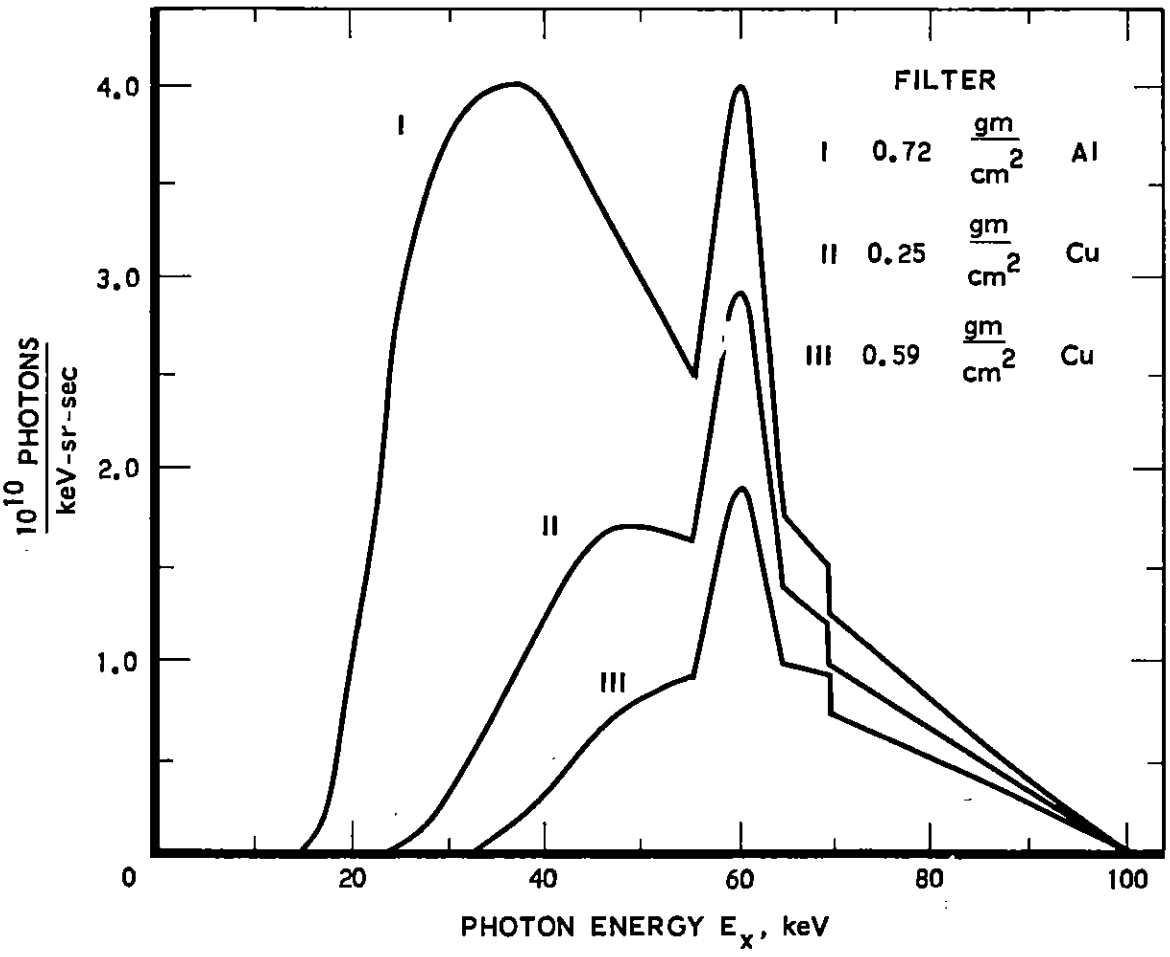

Fig. 2. X-Ray Spectra from 100-kV, 1-mA X-Ray Tube Used for Photoemission Studies

III. EXPERIMENTAL RESULTS

Thin metal sheets available in our laboratory were: foils of Al, Ti, Fe (stainless steel), Cu (brass), Ag, and Ta; some thicker sheets of Mg, pure Cu, and Pb; and some very thin gold leaf. Thicknesses of the irradiated samples are given in Table 1. Ideally, the foil should be thicker than an electron mean path length S_e, but still be thin compared to a radiation attenuation distance. Representative values for S_e are also given in Table 1. In addition, a few samples of dielectric sheets were tested. It was found that the photoemission from a dielectric backed by the conducting carbon was about the same as from a metal sheet when a large negative retarding potential was applied. Other results for dielectrics are not discussed here. No special cleaning procedures were used on the metal surfaces other than to use fine emery cloth on the thicker samples and to wipe off most of the samples with acetone. It was necessary to remove any unknown coatings from the emitters. For instance, the photoemission yield from one sample of lead was about 30% lower than that from the other samples until a silvery-appearing coating was rubbed off with emery cloth.

First, let us consider how bias voltages on the retarding grid change the measured photocurrents. Typical results are displayed in Fig. 3 where it may be noted that a negative bias of only -20 volts was sufficient to retard the low-energy secondaries from metals. Moreover, the emission current was not further reduced at higher bias voltages. It is also interesting to observe that a positive bias voltage pulled many additional electrons away from the emitter, particularly for the graphite. The contribution of secondary electrons was defined to be the percentage increase in the photocurrent with zero bias voltage relative to the photocurrent with negative bias (usually -500 volts). These secondaries added 20 to 30% to the photocurrent for the soft spectrum (I) and 10 to 20% for the two harder spectra (II and III). In our previous pulsed photoemissions, the secondary-electron contribution appeared

Table 1. Emitter Parameters and Measured Photoemission for Spectra I, II, III

Material	z	S_e at 60 keV (mgm/cm^2)	Thickness (mgm/cm^2)	Av j_e (10^{-13} A/cm^2)			Error (%)
				I	II	III	
C	6	6.6	340.0	0.093	0.028	0.013	±25
Mg	12	7.6	73.0	0.97	0.33	0.16	±8
Al	13	7.8	4.8 6.9	1.15 1.20	0.35 0.39	0.17 0.19	±8
Ti	22	8.6	2.3 4.4	4.2 5.3	1.06 1.63	0.44 0.76	±6
Fe	26	9.0	3.9	8.1	2.72	1.26	±5
Cu	29	9.4	22.5	10.3	3.57	1.75	±5
Ag	47	10.8	13.1	20.0	8.7	4.4	±5
Ta	73	13.0	8.4	26.3	9.7	5.0	±5
Au	79	13.3	0.4	6.1	---	---	±7
Pb	82	13.6	1100.0	31.0	11.3	5.7	±5

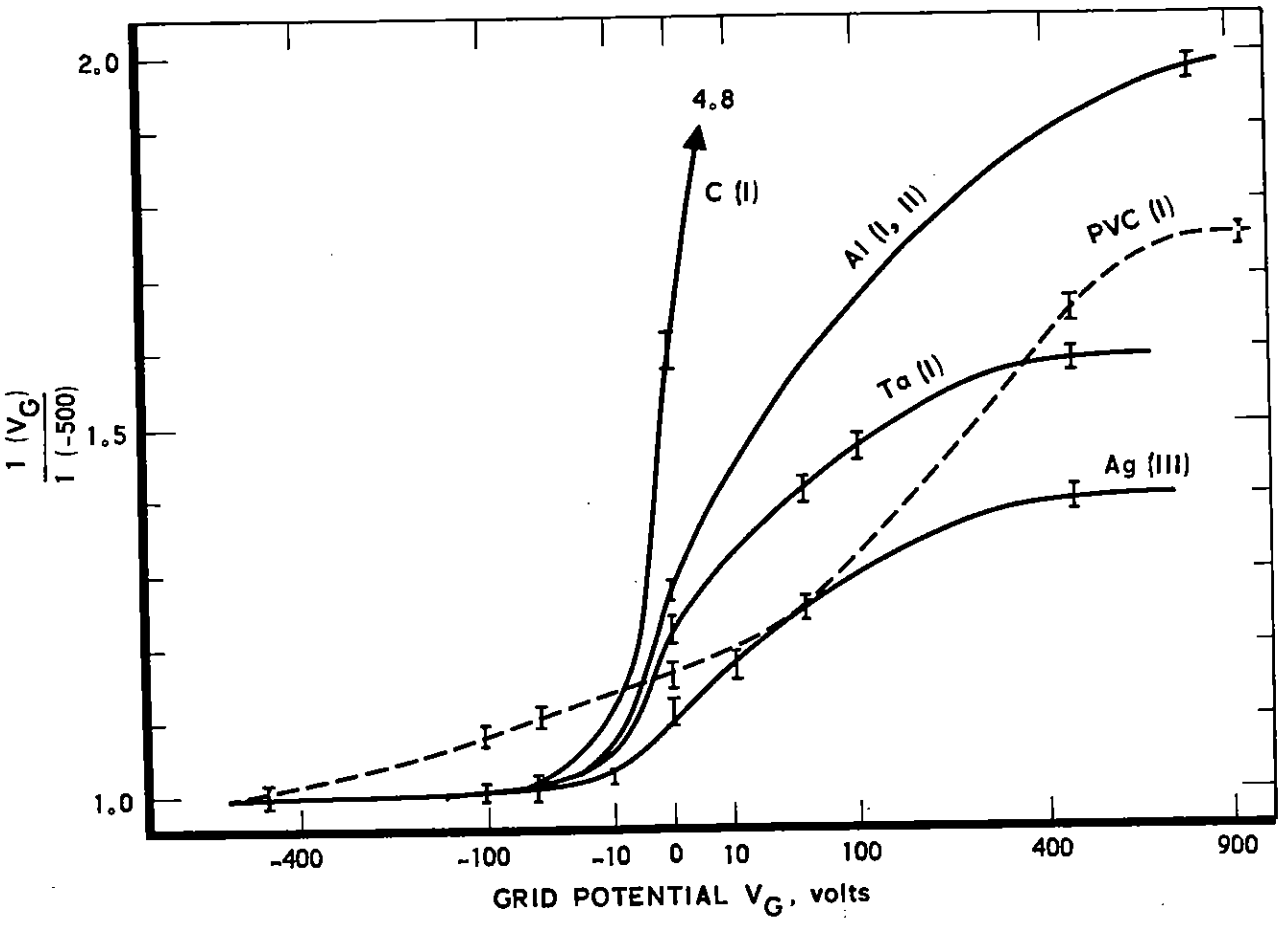

Fig. 3. Normalized Photoemission Current as a Function of Bias Voltage on Retarding Grid (Wire grid is 100% transparent to incident radiation and 95% transparent to emitted electrons.)

to be more than twice as large as that measured here.[2] This discrepancy can be explained by geometric differences in the test setups when we examine the results in Fig. 3. In the previous pulsed study, closely spaced parallel plates were used and, thus, an applied bias always produced a positive field on one of the two plates. Furthermore, since one of these plates was graphite, the present results show its photoemission was very high with a positive field.

In order to determine an accurate value for the forward and backward photoemission from each metal surface, it was necessary to subtract the contribution from the exposed surface of graphite. The magnitude of the carbon photoemission was obtained from irradiation of just the graphite target itself and was found to be negligible compared to photoemission from surfaces with $z > 22$. On the basis of results from other low-z emitters such as aluminum, half the measured current was assumed for each graphite surface at oblique incidence, while for normal incidence 2/3 was assumed to go in the forward direction and only 1/3 in the backward direction. Radiation angles of incidence, relative to the surface normals, were $\theta = 0$, 30, 45, 60, 70, and 80 deg, and typical data are shown in Fig. 4. As previously mentioned, a major uncertainty in each data point came from variations in the x-ray output. The data presented have been normalized to correspond to the same irradiated area of 8.0 cm^2 at all angles of incidence. In the case of the wide samples, the measured currents were multiplied by $\cos \theta$ to compensate for the increase in the irradiated area at oblique incidence. Similarly, the measured currents from the narrow samples were corrected for small variations in the irradiated area. After this normalization, there was no significant difference in the results obtained with the two widths of target foils.

As expected, the photoemission currents had the highest and lowest values at normal incidence in the forward and backward directions respectively. At an increased angle of incidence, the forward and backward photoemission should, in principle, tend toward the same value. This trend was

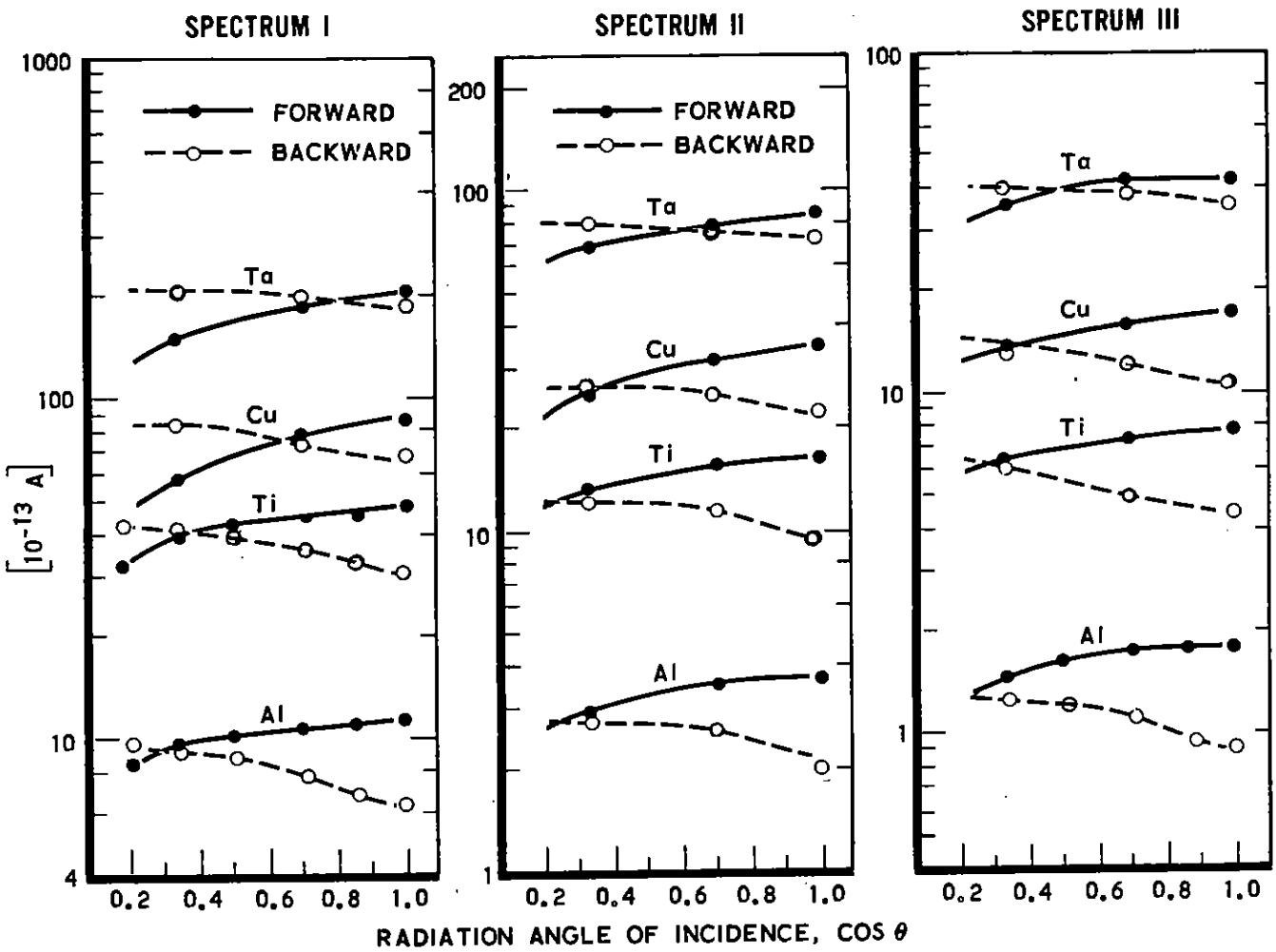

Fig. 4. Photoemission Currents from 8 cm^2 of Emitter Surface as a Function of Radiation Angle of Incidence (All data for V_g = -500 volts.)

observed up to about 60 deg, and then the forward emission started to fall off because of increased radiation attenuation in the metal foil. Attenuation in the graphite support was calculated to be less than in any foil. It should be noted that the sum of forward and backward emission at normal incidence was usually slightly less than the corresponding sum at oblique incidence. This slight decrease will be considered later in the comparisons of the relative magnitude of photoemission from different metals. As expected, the forward-to-backward ratio of photoemission decreases as z increases, ranging from 1.9 for Al to 1.1 for Ta. It was also expected that this forward-to-backward ratio would increase for the harder spectra, but this trend was very slight. In the few cases where foils much thinner than an electron mean path length were measured, notably Ti, Fe, and Au, the forward-to-backward ratios were not significantly higher except in the case of the very thin gold leaf. However, the magnitude of the photoemission from these thin samples was reduced. One special sample of copper was studied where the surface was greatly roughened by indentations formed by pressing a file against the surface. In this condition, the photoemission did not vary with angle of incidence, as might be expected.

The relative magnitudes of the photoemission currents from the different metal surfaces must be considered next. Since we are interested in comparisons of the primary-electron emission with theory, only the measured photoemission currents with a negative bias are used. A nominal average value for the photoemission from a single surface of each material was assumed to be the backward emission near grazing incidence. Note in Fig. 4 that the average of the forward and backward emissions for radiation incident around 45 deg results in about the same value as the backward emission at grazing incidence. For the lower-z emitters, the average of the forward and backward photoemissions at normal incidence was 5 to 10% lower than at oblique incidence. Values of the average emission current densities (10^{-13} A/cm^2) are listed in Table 1 for the three irradiation spectra. We see that the

photoemission from the thinner sample of titanium is lower than that from the thicker sample and that the discrepancy becomes larger for the harder spectra. The extreme thinness of the gold leaf resulted in a greatly reduced photoemission relative to the other high-z foils. The average emission current densities (10^{-13}A/cm^2) are plotted in Fig. 5 for the thicker samples. Except for the previously mentioned sample of lead, the photoemission from various samples of a given material appeared to be the same within experimental error.

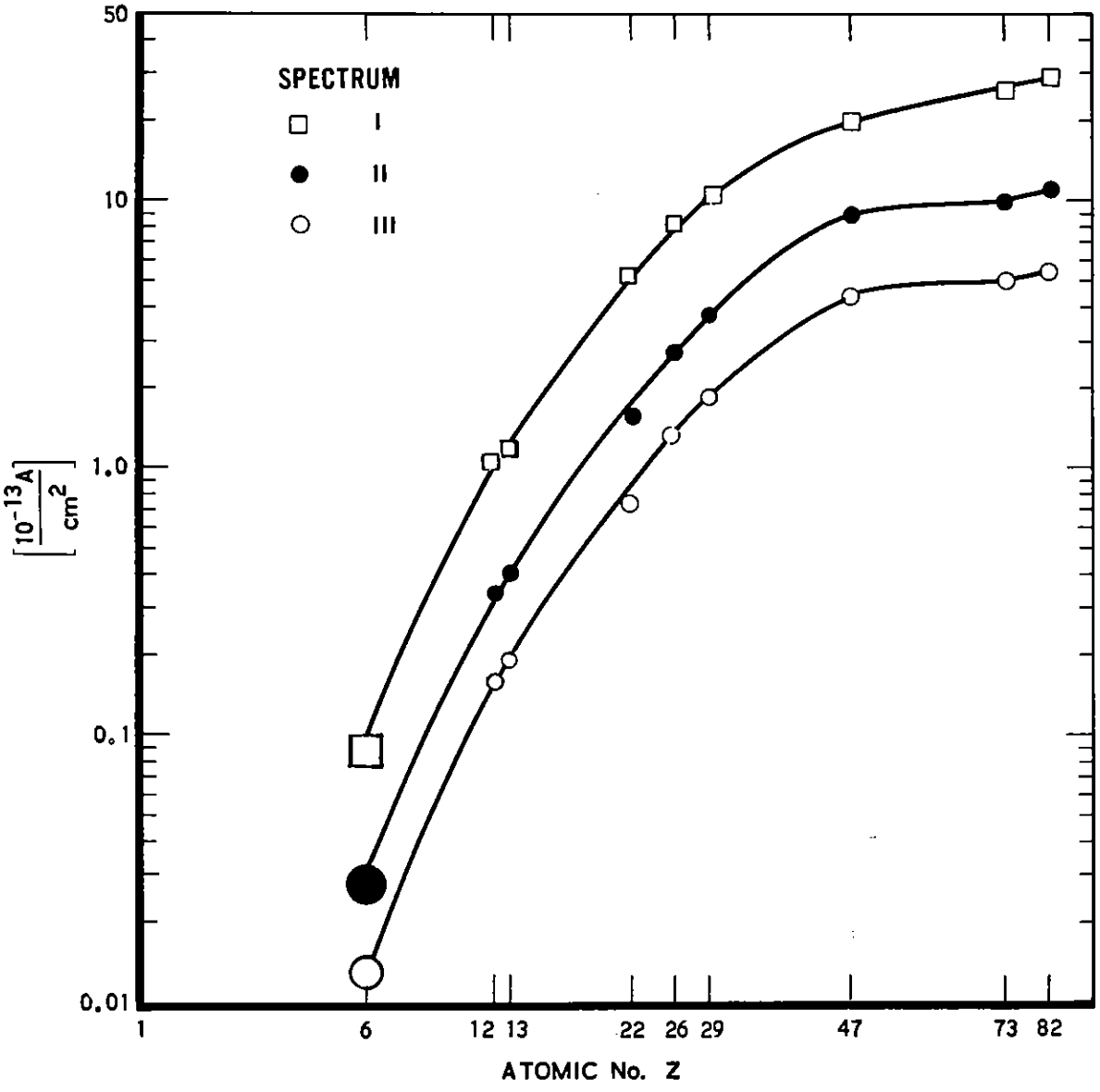

Fig. 5. Average Photoemission Current Densities j_e from Metal Foils for Radiation at Oblique Incidence

IV. ANALYSIS

Let us assume that, at each photon energy E_x, the electrons emitted from a surface are all generated within a layer having a thickness S_e, which is expressed in gm/cm^2. If n_x is the number of photons with energy E_x incident on this layer, then the number of electrons n_{ec} created in this layer is given by $n_{ec}/n_x = 1 - \exp(-\mu_a S_e)$ where the photon energy-absorption cross section μ_a is expressed in cm^2/gm. It is well known that the product $\mu_a S_e$ is much smaller than unity for all photon energies of interest, and thus $n_{ec}/n_x = \mu_a S_e$. Next we assume that only a fraction G_e of the electrons created in the layer are emitted, and so the photoelectric yield at each photon energy can be expressed by

$$n_e/n_x = \mu_a S_e G_e \qquad \text{electrons/photon} \tag{1}$$

where $G_e < 1$ is a dimensionless constant that takes into account both geometric effects and electron scattering in determining how many electrons n_e actually escape. Actually, the right-hand side of Eq. (1) should be divided by cos θ to account for an increase in the photoelectric yield at oblique incidence of the radiation. However, since we are really interested in the number of emitted electrons per unit area, there is a corresponding cos θ reduction of the photon flux at oblique incidence. In this analysis, we define S_e to be the average path length of an electron, since that is the greatest depth from which an emitted electron could originate. (Of course, when straggling is considered, a very few electrons emerge from greater depths.) For the present range of photon energies, the factor G_e is assumed independent of photon energy and depends only on the material and the radiation angle of incidence. If one used an electron range R_e in Eq. (1) instead of the electron path length S_e, the appropriate values for the geometric factor would differ considerably from G_e.

In the present work, all electrons were generated by the photoelectric effect except for a few by Compton scattering in the lowest-z materials. It is well known that such photoelectrons tend to have initial velocity vectors mostly at right angles to the direction of the incident photons. But, owing to momentum conservation, the average initial electron direction is slightly canted in the direction of the photons and this directional anisotropy increases for higher photoelectron energies. As a result, the forward emission of electrons from a surface will exceed the backward emission. Of course, we are neglecting here any attenuation of the radiation passing through a material to produce forward emission. The anisotropy of forward to backward electron photoemission from a surface depends not only on the initial velocity distribution, but also on the effects of electron scattering in the material. As we observed, the measured ratio of forward to backward emission at normal incidence was only 1.1 for the high-z emitters such as Ta and increased to less than 2 for Al and Mg. Thus, although the value of G_e in Eq. (1) does depend on the radiation angle of incidence, it only varies by up to ±35% from some average value.

Let us now consider only average values of G_e for calculations of the average photoemission currents. To compute the average emission current density, Eq. (1) becomes

$$j_e = e \sum_{E_x} n_e = G_e \, e \sum_{E_x} n_x \sum_{K, L, M} \mu_a \, S_e \qquad (2)$$

where the first sum is over the irradiation spectrum and the inner sum is over the different electron binding energies. This second sum arises because an electron path length (or range) depends on the initial electron energy, which is the difference between the photon energy and the appropriate binding energy. For the case of Compton electrons, a similar

summation over electron energies must be made. Values for μ_a were the photoelectric cross sections[4] augmented by the energy-absorption portion of the Compton cross section when necessary.* Values for the electron mean path lengths S_e were taken from the tabulations of Berger and Seltzer who used a continuous slowing-down approximation to compute so-called c.s.d.a. ranges.[5] Although their computed values are named c.s.d.a. ranges, they are specified to be path lengths and not rectilinear ranges. In addition, they also state that real electron path lengths will have an average value somewhat longer than the c.s.d.a. value because of straggling. For the energy range of 10 to 100 keV, it remains to be determined by how much the average values of real electron path lengths exceed the computed values.

To obtain computed electron fluxes for several of the emitting metal surfaces, the summations of Eq. (2) were carried out with the three irradiation spectra of Fig. 2 divided into 10-keV intervals. The results of these summations were multiplied by the appropriate solid angle and then divided into the average measured values of j_e to give the values of G_e presented in Table 2. Considering the 5 to 20% accuracy of the measured values, there is a remarkable consistency among the derived values for the three irradiation spectra. The average values of these derived G_e factors are plotted in Fig. 6 where the dashed line is an arbitrary fit to the data. For 30-keV photons, the corresponding average photoemission yields are: 5.1×10^{-4} for Al, 4.0×10^{-3} for Cu, and 9.1×10^{-3} for Ta. There is very little in the open literature in the way of experimental or theoretical results with which to compare our values in a straightforward fashion. For instance, Bradford[1] reports the differential quantity photoelectrons/photon-sr for a broad spectrum

*Other tabulated values agree to better than 10%.

[4]W. H. McMaster, N. K. del Grande, J. H. Mallett, and J. H. Hubbell, Compilation of X-Ray Cross Sections, UCRL-50174, Lawrence Radiation Laboratory, Livermore, California (May 1969).

[5]M. J. Berger and S. M. Seltzer, "Tables of Energy-Losses and Ranges of Electrons and Positrons," Studies of Penetration of Charged Particles in Matter, National Research Council Publ. 1133, 205 (1964).

Table 2. Average Photoemission Coefficient $\bar{G}_e$

Emitter	$\bar{G}_e$ Values		
	Spectrum I	Spectrum II	Spectrum III
C (graphite)	0.37 ± 0.06	0.38 ± 0.08	0.35 ± 0.10
Mg	0.29 ± 0.03	0.32 ± 0.03	0.34 ± 0.04
Al	0.28 ± 0.03	0.30 ± 0.03	0.32 ± 0.04
Ti	0.22 ± 0.02	0.22 ± 0.02	0.22 ± 0.02
Cu (brass)	0.22 ± 0.02	0.22 ± 0.02	0.22 ± 0.02
Ag	0.22 ± 0.02	0.21 ± 0.02	0.19 ± 0.02
Ta	0.18 ± 0.02	0.18 ± 0.02	0.19 ± 0.02
Pb	0.17 ± 0.02	0.16 ± 0.02	0.16 ± 0.02

peaked at 30 keV. MacCallum and Dellin[6] have computed the bulk photocurrents within a material, and state the values can be used to estimate an upper limit for the photoemission at a vacuum interface. We have compared their values with our own photoemission yields for normally incident 30-keV photons. The forward emission that we measured from Al, Cu, and Ta results in yields of 6.2×10^{-4}, 4.4×10^{-3}, and 9.4×10^{-3} respectively, while MacCallum and Dellin[6] quote values of 5.4×10^{-4}, 5.1×10^{-3}, and 14.1×10^{-3}. They have also computed the ratios R_p/S_e where R_p is the penetrating range defined as the average distance an electron travels in its initial direction within the bulk material. It is to be emphasized that this

[6] C. J. MacCallum and T. A. Dellin, "Photo-Compton Currents in Unbounded Media," J. Appl. Phys. 44, 1878 (1973).

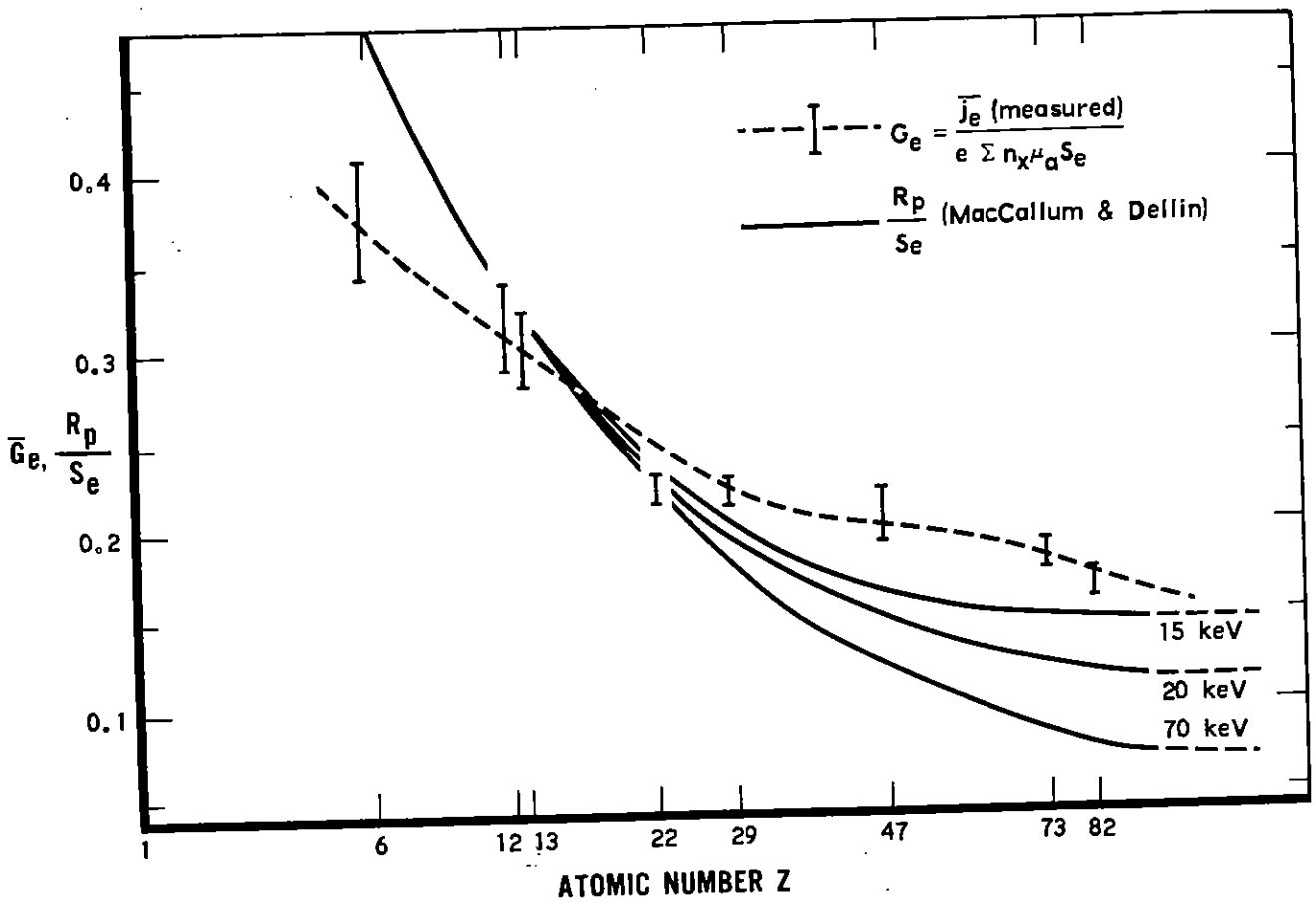

Fig. 6. Average Photoemission Factors G_e for Metal Foils as a Function of Atomic Number z (Dashed line is the estimated smooth fit to the data. The computed ratios of electron mean penetration R_p to the mean path length S_e at different electron energies are given for comparison although this ratio is defined differently from G_e.)

ratio is not expected to be the same as G_e, but it is nevertheless interesting to compare the similar magnitudes and z-dependences in Fig. 6. Both quantities are observed to decrease for higher-z materials, showing the increased effect of multiple electron scattering. The factor G_e does not decrease so rapidly as R_p/S_e because R_p is determined by the end positions of the electrons, while photoemission depends on the intersection of electron paths with the emitter surface.